Quel est l'impact de simplifications géométriques et d'homogénéisations sur la modélisation du comportement hydromécanique d'un affleurement rocheux calcaire poreux et fracturé ?

Alain Thoraval, Frédéric Cappa, Y. Guglielmi

Impact of simplifications on the modeling of the hydromechanical behavior of a fractured porous carbonate outcrop

Alain Thoraval[*] - Frédéric Cappa[**] - Yves Guglielmi[***]

[*] *Institut National de l'Environnement Industriel et des Risques (INERIS), Parc de Saurupt - CS 14234 - F-54042 Nancy, France. e-mail: alain.thoraval@ineris.fr*
[**] *GeoAzur (UMR6526), U. de Nice Sophia-Antipolis, 250 rue Albert Einstein, Les Lucioles 1, F-06560 Sophia-Antipolis, France. e-mail: cappa@geoazur.unice.fr*
[***] *U. de Provence, Laboratoire de Géologie des Réservoirs Carbonatés, 3 place Victor Hugo, Marseille cedex 3, France. e-mail: yves.guglielmi@univ-provence.fr*

ABSTRACT. *This paper presents a numerical analysis of in-situ well injection and pumping experiments carried out at the Coaraze Laboratory site with simultaneous fluid pressure and rock deformation measurements in boreholes. The Coaraze site is a small fractured and porous carbonate reservoir (decametric scale) that outcrops 30 km north of Nice. We have developed three-dimensional numerical approaches to simulate the hydro-mechanical behavior of major fractures and the surrounding equivalent continuous and porous medium that represents the intact rock and the other fractures. We have particularly focused on evaluation of the impact of geometrical simplifications and up-scaling on the quality of the prediction of the reservoir hydro- mechanical behavior during hydraulic experiments. Including in the model a few "key" fractures that have important roles in fluid flow and deformation are shown to be as efficient as performing an up-scaling of the fracture network.*

RÉSUMÉ. *Cet article présente une analyse numérique de résultats d'essais d'injection et de pompage réalisés dans le site laboratoire de Coaraze avec mesures simultanées en forage de variations de pressions hydrauliques et de déformations. Le site de Coaraze est un petit réservoir calcaire poreux et fracturé (échelle décamétrique) qui affleure à une trentaine de kilomètre au nord de Nice. Nous avons développé des approches tridimensionnelles pour simuler le comportement hydromécanique des fractures les plus importantes couplé avec celui d'un milieu poreux équivalent représentant la matrice rocheuse intacte et les autres fractures. Nous avons, en particulier, évalué l'impact de simplifications géométriques et d'homogénéisations sur la qualité des prédictions du comportement hydromécanique du réservoir durant les expérimentations. Inclure dans le modèle uniquement les fractures "clef", jouant un rôle important hydrauliquement et/ou mécaniquement, s'avère aussi efficace qu'exécuter une homogénéisation prenant en compte l'ensemble des fractures.*

KEYWORDS: *Hydro mechanical couplings, fractured porous rock, in-situ measurements, up-scaling, equivalent properties, numerical modeling,3DEC, FLAC[3D].*

MOTS-CLÉS : *Couplage hydromécanique, roche fracturée poreuse, mesures in situ, homogénéisation, propriété équivalente, modèle numérique,3DEC, FLAC[3D].*

1. Introduction

Forecasting the hydromechanical behavior of a fractured rock mass is still of ongoing interest, and has indeed been stimulated by the growing concern of national and local governments about the safety of people and property. This concern has focused environmental protection on issues such as the stability of rocky slopes, the sealing of underground storage sites (hydrocarbon, radioactive and industrial waste, greenhouse gases), the efficiency of the geothermal concept, and the transport of pollutants. In all cases, hydromechanical couplings that occur in fractured media can affect the fluid flow and mechanical deformation processes. The overall objectives are therefore to predict the behavior of fractured rock masses from both the mechanical point of view (i.e. evaluation of the risk of instability), and the hydraulic point of view (i.e. flow assessment through storage).

Most of the time, modeling large-scale hydromechanical behavior of a fractured rock mass requires a preliminary up-scaling of the rock-mass properties, for reasons related both to difficulties in performing exhaustive fracture measurements and to computer code limitations (Pouya *et al.*, 2009; Blum *et al.*, 2009). After an up-scaling has been achieved, simulations on a large scale can then be performed, with any computer code simulating the hydromechanical behavior of a porous medium. Therefore, in large-scale analyses, a combination of the continuum approach and the discrete approach at appropriate scales can be particularly effective in representing fracture effects on the behavior of fractured rock masses. Various up-scaling techniques exist in the literature to determine the equivalent permeability tensor, and the stiffness tensor defining the relationships between stresses and strains (Oda, 1986; Ababou, 1991; Min *et al.*, 2004; Thoraval *et al.*, 2004).

Many key questions arise with the modeling of fluid flow and mechanical interactions in a fractured porous reservoir, such as: Which fracture network geometry should be considered? To model the local fracture hydromechanical response, should other fractures in the vicinity be introduced? Do these additional fractures have to be introduced explicitly, or can they be introduced through an equivalent continuous porous medium representation? Does the rock-matrix poroelastic behavior significantly affect the rock-mass response, or is it possible to neglect it?

In the present study, we examined the impact of various simplifications on the prediction of the hydromechanical behavior of a fractured and porous rock mass subjected to hydraulic loadings. A three-dimensional numerical approach was developed, which deals with the hydromechanical behavior of both the porous rock matrix and the fractures. Simulations were compared with experimental data from long-duration injection and pumping tests performed at the Coaraze Laboratory site in France. The analysis of the various modeling options performed leads us to specify some methodological recommandations regarding the development of predictive models that are suitable for hydromechanical simulations of fractured and porous rock masses.

2. The Coaraze in-situ experiments and previous modeling data

2.1. *An overview of the Coaraze Laboratory site*

The study that we present here is based on experiments carried out at the Coaraze Laboratory site in southern France, 30 km north of the city of Nice. This site was developed for in-situ studies of hydromechanical processes in fractured carbonate rocks. The site is a small fractured reservoir (30 m × 30 m) in a surface outcrop that is made up of a 15-m-thick succession of low porosity limestone (figures 1a and 1c). The hydraulic boundaries of the reservoir are well constrained, with impervious layers at the bottom and the top, an impervious fault located down-stream towards the southwest, and an exposed rock slope that is surface sealed by impervious grout to a height of about 10 m. Upstream, towards the northeast, a permeable fault allows water to flow continuously into the reservoir.

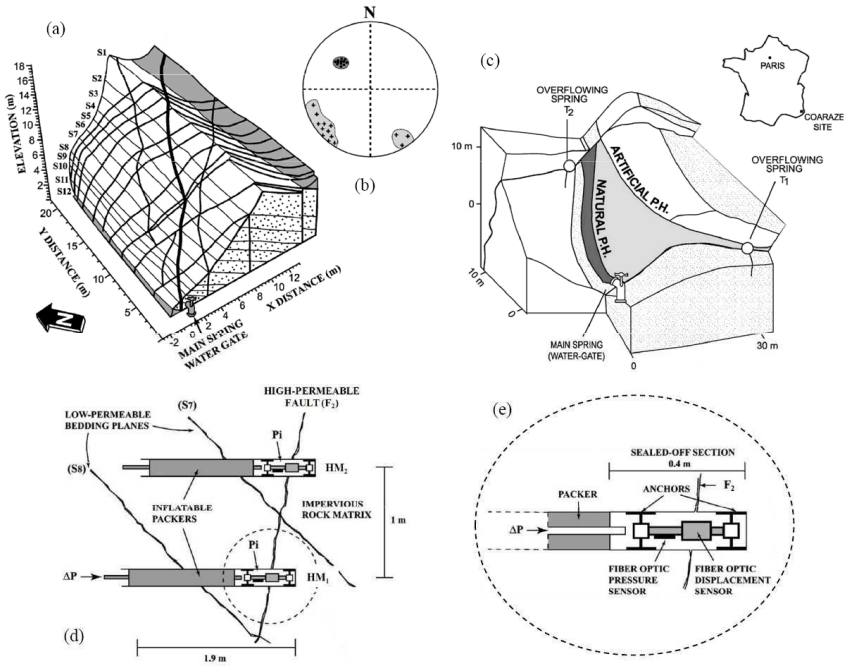

Figure 1. *Coaraze laboratory site. (a) Three-dimensional view of the large continuity fractures; (b) Pole plots showing brittle faults and bedding-plane orientations (lower hemisphere); (c) Block diagram showing water table variations induced by opening/ closing the gate; (d) Instrumented fracture for the injection and pumping experiments; (e) Detailed view of the pressure and deformation coupled measurement in the fracture.*

The rock mass is naturally drained by a spring located in the southwest corner (figure c). For the experimental studies, the spring was artificially closed with a water gate that allowed control of the piezometric level in the reservoir.

Inside the reservoir, changes in fluid pressure and deformation were simultaneously monitored at single discontinuities and in the rock matrix. In the experiment that is modeled in this study, two horizontal boreholes (figures 1d and 1e - HM_1 and HM_2) that were spaced 1 m apart vertically were drilled normal to a sub-vertical fault F_2 (figure 1d); each borehole terminated 5 cm beyond the fault. In each borehole, the fault was isolated with an inflatable packer, to create a 0.4 m long sealed section. In each sealed section, the measurement device consisted of a fiber-optic fluid pressure and a fiber-optic normal displacement sensor fixed to the borehole walls by two anchors that were located on either side of the fault. This device was adapted from the BOF-EX device developed by RocTest-Telemacs (Cappa *et al.*, 2006-a). The borehole equipment was capable of simultaneously measuring changes (with high frequency [120 Hz] and high accuracy) in fluid pressure (±1 kPa) and displacement normal to the fault walls ($\pm 1 \times 10^{-7}$ m) during the hydraulic tests.

Previous modeling studies (Cappa *et al.*, 2005, 2006-b, 2008; Guglielmi *et al.*, 2008) have evaluated and improved the conceptual models used to simulate the hydromechanical behavior of a fractured rock mass. It has been shown (Guglielmi *et al.*, 2008) that the response of the overall model is highly sensitive to the inclusion of major discontinuities (vertical faults, in the case of the Coaraze site). The simplification of other fractures (including bedding planes) by an equivalent porous rock mass is broadly acceptable in the short term, with the fault explaining 90 % of the movements measured. However, it can lead to important errors in local predictions.

2.2. *Geometrical characterization of the fracture network*

The preliminary studies carried out on the site by Guglielmi (1999) showed that the fracture network of the Coaraze site consists of three principal sets of discontinuities (figures 1a and 1b): three faults with a N50 to N70 trend, a dip angle of 70° to 90° towards the NW (F_{11}, F_{12} and F_{13}), and with a 2-3 m spacing; eleven faults with a N120 to N140 trend, a dip angle of 75° to 90° towards the NE (F_1–F_{10} and F_{14}), and with 2 m spacing; twelve bedding planes with a N40 trend, a dip angle of 45° towards the SE (S_1–S_{12}), and with 0.5-1.0 m spacing.

An accurate mapping of the fracture network was carried out with an electronic distance-meter (i.e. Leica TDA5005). The measurement consisted of positioning the electronic distance-meter in front of the outcropping faces of interest of the reservoir, and measuring the spatial coordinates (X, Y, Z) of points located along the fracture intersections with the topographic surface. About 500 measurements were

performed in all, with some fractures characterized by more than twenty points. Each series of measurements provided a progressive improvement to the geometrical model (new measurements are often being conditioned by the model confrontation with the ground observations). The final result was the exhaustive three-dimensional mapping of the main fractures cutting the reservoir.

2.3. *Hydromechanical experiments*

The experiments analyzed in this study were constant step rate pumping tests (i.e. the flow rate was kept constant) and injections (i.e. the pressure was kept constant) in a borehole intersecting the major fracture F_2 (figure 1d). Each step lasted 30 min to 1 hour. Fluid pressure and fracture deformation measurements were carried out at each step in the injection/ pumping borehole HM_1 and in an adjacent monitoring borehole HM_2. The measurements indicated (figure2) that:

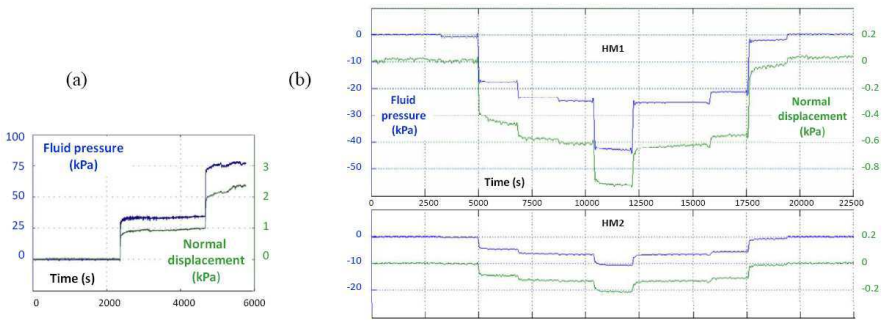

(c)	Measurements at HM_1			Measurements at HM_2	
	Flow rate (l/s)	**Hydraulic pressure variation (kPa)**	**Normal displacement variation (µm)**	**Hydraulic pressure variation (kPa)**	**Normal displacement variation (µm)**
Injection test	0	**0**	0	0	0
	+0.61	**+36**	+1.31	+7.8	+0.44
	+1.33	**+78**	+2.85	+9.1	+0.96
Pumping test	**0**	0.00	0.00	0.00	0.00
	-0.05	-2.97	-0.11	-0.64	-0.04
	-0.44	-26.21	-0.95	-5.62	-0.32
	-0.51	-30.40	-1.10	-6.51	-0.37
	-0.55	-32.79	-1.19	-7.02	-0.40
	-0.77	-44.88	-1.63	-9.60	-0.55
	-0.55	-32.79	-1.19	-7.02	-0.40
	-0.52	-31.00	-1.12	-6.64	-0.38
	-0.46	-27.41	-0.99	-5.87	-0.33
	-0.09	-5.35	-0.19	-1.15	-0.06

Figure 2. *Hydraulic pressure and normal displacement curves relative to injection (a) and pumping (b) tests; (c) Synthetic table of pressures and displacement values measured at HM_1 and HM_2 at each pumping and injection step*

– during the injection test, the pressures reached 36 kPa for the first injection step, and 78 kPa for the second step. These pressures corresponded to injected flow rates of 0.61 l/s and 1.30 l/s at HM_1, respectively, and an associated normal opening of the fracture of 1.00 mm and 2.35 mm, respectively. At HM_2, the measured pressure variations were 7.8 kPa and 9.1 kPa, respectively (figures 2a and 2c). The normal displacements in HM_2 were not monitored because the sensor was temporarily out of order;

– the pumping applied induced hydraulic pressure variations and the associated normal closing of the fracture at HM_1 and HM_2. It appeared that a pumping flow rate of 0.77 l/s was needed to reduce the hydraulic pressure to zero at HM_1. The pumping induced the maximum normal closing of the fracture of 0.9 mm at HM_1 and 0.2 mm at HM_2, respectively (figures 2b and 2c).

3. Choice of a model for experimental interpretation

3.1. *Hydromechanical model with only fracture porosity*

In this model, the matrix porosity was ignored, and it was assumed that the flow occurred only through the fractures taken into account in the model. The numerical models were run using version 4.10 of the distinct element 3DEC commercial software (Itasca Consulting Group, 1994).

3.1.1. *Building the "reference" hydromechanical model with 3DEC code*

A small model (8 m × 8 m × 8 m) was imported from the scale geometrical model of the site, and it was centered on the test borehole HM_1 (figure 3 - model C). The plurimetric fractures included were: the instrumented fracture R_4; the bedding planes S_{10}, S_9, S8 and S_7 ; the fractures R_{20}, R_{9b} and R_{9a} (that are intersecting the boreholes) ; the fracture J_1, J_2, D_6, and R_{10b} (that are not intersecting the boreholes).

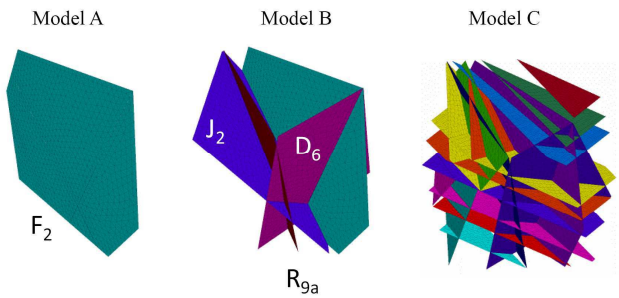

Figure 3. *3DEC model geometries*

The rock matrix is impermeable and has an elastic behavior. The fractures have a linear elastic behavior. The fracture stiffness variation is assumed to be negligible during the test, because of the small magnitude of the measured displacement. The flow in the fractures follows the cubic law.

3DEC allows simulation of the hydromechanical behavior of a deformable and impermeable matrix cut by fractures that are presumed to be saturated with water. The flow in the fractures is regarded as laminar, and it is governed by the cubic law (Witherspoon *et al.*, 1981). Hydromechanical calculations assume a relationship between the fracture hydraulic opening variations ($a - a_0$) and the mechanical closing variation (Δu_n), where a0 is the hydraulic opening at the initial state before the test, and the mechanical closing variation (Δu_n) is obtained by dividing the effective normal stress variation ($\Delta \sigma_n'$) by the fracture normal stiffness (K_n). The variation of the effective normal stress is obtained by withdrawing the hydraulic pressure variation from the total normal stress variation, according to Terzaghi's law for effective stress (Terzaghi, 1923).

The values of the model input data were adjusted to best fit the pressure/ displacement measurements: properties of the rock matrix: *density* (ρ) = 2400 kg/m^3, *Young modulus* (E) = 40 GPa, *Poisson's ratio* (ν) = 0.3; properties of the fracture: *normal stiffness* (k_n) = 5 GPa/m for the sub-vertical fracture and 50 GPa/m for the bedding planes, *tangential stiffnesses* (k_s): ten-fold weaker, *hydraulic apertures* (a_0) = 5×10^{-4} m for the sub-vertical fracture and 10^{-4} m for the bedding planes.

The model was initially fully saturated (after closing the water-gate, figure 1c), with initial water pressures consistent with the measured values of 45 kPa at HM_1 and 33.3 kPa at HM_2.The distribution of the initial stress was more complex to estimate, as it depended in particular on the geometry of the topographic surface and of its fracturing. This was roughly estimated through regional-scale mechanical modeling of the valley in which the site is nested (Cappa *et al.*, 2006-b). This simulation allowed estimation of the initial stress field at any point in the hydromechanical model; indeed, the initial total normal stress to the fracture at point HM_1 was approximately σ_{ni} = 120 kPa (such that σ'_{ni} = 120 - 45 = 75 kPa). The simulations consisted of fixing the values of pressure (injection tests) or flow (pumping test) imposed during the field experiments at the injection/ pumping point HM_1. At each step, the equilibrium state was computed.

The variations computed at points HM_1 and HM_2 are given in table 1 for both the injection and pumping test simulations. A comparison of the computed values for model C with the measurements shows that the model correctly predicts both the flow-rate at HM_1 when a hydraulic pressure is imposed, and the pressure at HM1 when a flow rate is imposed (less than 12 % difference with the measurements). The normal displacements for the fracture at HM_1 are predicted by the injection-test simulation with less than a 20 % overestimation. This overestimation is higher (80 %) in the case of the pumping-test simulation. This might be related to the fracture stiffness decrease that accompanies the effective normal stress decrease, as

has been shown in many laboratory tests. Indeed the simulations assume constant stiffness values in both cases. Then, during the injection stage, the effective stress decrease related to the increase in the hydraulic pressure into fracture F_2 results in induction of a normal stiffness decrease in fracture F_2. In contrast, during the pumping stage, the effective stress increase related to the decrease in the hydraulic pressure into fracture F_2 results in induction of a normal stiffness increase in fracture F_2. The hydraulic pressure variations at HM_2 are correctly predicted by the pumping-test simulation (less than a 13 % difference from the measurements). However the pressures are strongly underestimated by the injection-test simulation. No clear explanations for these effects can be proposed here, although this might be linked to some error in the representation of the fracture network geometry, or to an effect of the hydraulic boundary condition. Indeed, because of the model size, the constant pressure boundary might artificially reduce the pressure variation at HM_2.

Geometry A: F_2 **Geometry B:** F_2, R_{9a}, J_2 and D_6 **Geometry C:** all the fracture		**Computed values at HM_1**			**Computed values at HM_2**	
		Flow rate (l/s)	**Hydraulic pressure variation (kPa)**	**Normal displacement variation (μm)**	**Hydraulic pressure variation (kPa)**	**Normal displacement variation (μm)**
1srt injection stage	**A**	0.530	+36	+1.27	+10.68	+0.54
	B	0.609		+1.28	+8.85	+0.51
	C	0.612		+1.31	+7.81	+0.44
2nd injection stage	**A**	1.153	+78	+2.75	+23.14	+1.18
	B	1.325		+2.77	+19.18	+1.10
	C	1.331		+2.84	+16.93	+0.96
1rt pumping stage	**A**	0.44	-30.37	-1.06	-8.85	-0.45
	B		-26.45	-0.93	-6.38	-0.37
	C		-26.34	-0.95	-5.59	-0.31
2nd pumping stage	**A**	0.55	-37.97	-1.33	-11.07	-0.56
	B		-33.06	-1.16	-7.98	-0.46
	C		-32.92	-1.18	-7.01	-0.40
3th pumping stage	**A**	0.77	-45	-1.57	-13.13	-0.67
	B		-45	-1.58	-10.87	-0.62
	C		-45	-1.62	-9.58	-0.55

Table 1. *3DEC computed hydraulic pressure and normal displacement values for different model geometries*

3.1.2. *Impact of reducing the fracture number in the model*

The effect has been explored by running two alternative models to the reference model, with their geometries distinguished according to the number of fractures introduced into the models (figure 3): model A (only the injected fracture F_2); model

B (only the fractures intersecting F_2: R_{9a}, J_2, D_6); model C (all of the fractures - reference case). In models A and B, no equivalent properties were given to the intact rock, which remained with the matrix properties.

In figure 4, comparing panels a, b and c, there is a decreasing of the hydraulic pressure in the injected fracture (especially around the injected point) if it is connected with other fractures. The surrounding fractures also impact on the normal displacement field (figures 4d and 4f). The normal displacement discontinuities clearly reveal the fracture traces on the injected fracture plane.

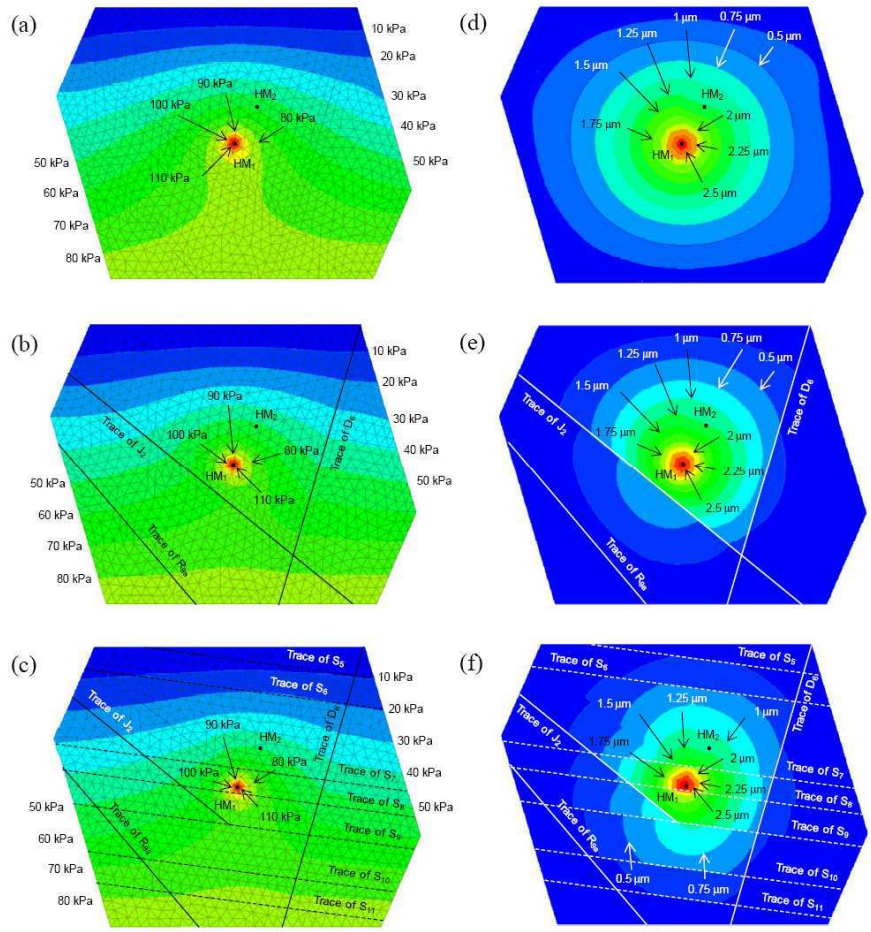

Figure 4. *Calculated hydraulic pressure and normal displacement fields within the injected fracture for the different 3DEC models geometries: (a) model A - hydraulic pressure; (b) model B - hydraulic pressure; (c) model C - hydraulic pressure; (d) model A - normal displacement; (e) model B - normal displacement; (f) model C - normal displacement*

The values of the hydraulic pressures, normal displacements, and flows in fracture F_2 at points HM_1 and HM_2 are given in table 1. The pressure variations between model with geometry A and the reference model C were computed considering the ratio of (value A – value C)/ value C. In the injection-test case, there is a 14 % decrease (from the reference case) in the calculated flow rate at HM_1, and a 37 % increase in the hydraulic pressure variation at HM_2 which are associated to a 3 % decrease in the normal displacement variation of the fracture walls at HM_1 and a 23 % increase at HM_2, respectively. In the pumping-test case, there are hydraulic pressure variation increases of 16 % at HM_1 and 60 % at HM_2; these are associated with decreases in the normal displacement variation of 13 % at HM_1 and 40 % at HM_2. The differences between models B and C are less important than the differences between models A and C. Indeed, for the flow rate, the hydraulic pressure variations and the normal displacement variations, the ratio (value B – value C)/ value C remains below 3 % at HM_1, and below 15 % at HM_2.

These data show that oversimplification of the model geometry (considering only the main fracture, but without up-scaling) can have an important impact on the hydromechanical response.

3.2. *Development of a double-porosity hydromechanical model*

A model was then developed that considered both of the flows through some fractures, and the flows within the blocks that were delimited by these fractures. Equivalent hydromechanical characteristics were given to each of the blocks to restore the hydromechanical behaviors of the initial porous and fractured rock mass that corresponded to this block volume. This model was built with version 3.10 of the FLAC^{3D} commercial software (Itasca Consulting Group, 2002). FLAC^{3D} was developed from Biot's theory of consolidation (Biot, 1941), and it was used in the fully coupled calculation mode. Changes in the variation of the fluid content were related to changes in pore pressure, saturation and mechanical volumetric strain.

3.2.1. *Reference model*

The FLAC^{3D} model geometry was imported from the 3DEC model geometry described previously (figure 5). Discontinuous fracture elements in 3DEC were changed into continuous 0.1-m-thick layers in FLAC^{3D}. Equivalent hydromechanical characteristics that represent the fractures and the matrix-block behavior were applied to these layers and to each block of the FLAC^{3D} model. In the reference model, which includes all of the fractures, the blocks were assumed to have the hydromechanical characteristics of the intact rock matrix.

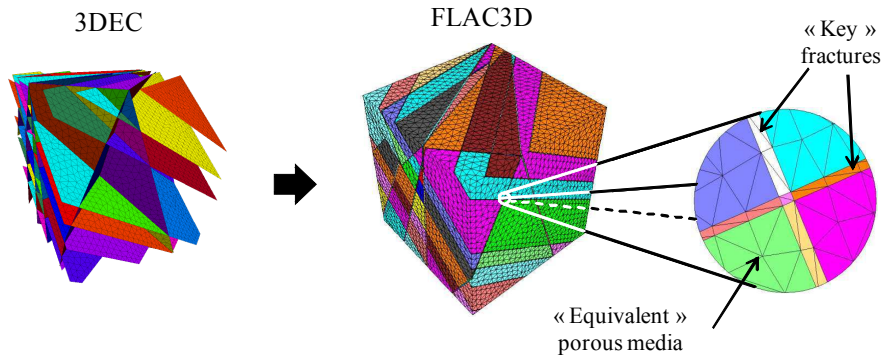

Figure 5. *Construction of the FLAC3D model geometry from the 3DEC model*

Equivalent hydromechanical characteristics for tabular zone represented the selected fractures: the mechanical behavior of the discontinuities was represented by associating a transversely isotropic model with the layers. The plane of isotropy corresponds to the fracture plane. The hydraulic behavior of discontinuities was represented by considering for the layer an intrinsic permeability equivalent to the permeability of a fracture. It can be shown that $k_{tabular\ zone} = a_0^3/12e$ [m^2], where a_0 is the initial fracture hydraulic aperture and e the thickness of the layer. The previous relationships made it possible to transform the previous 3DEC models into FLAC^{3D} models with the same hydromechanical response to the injection, as long as the matrix blocks between the fractures were assumed to be impervious, in both cases.

Equivalent hydromechanical characteristics for the porous block (cut by the selected "key" fractures) represented the intact matrix and the non-selected fractures: We have used the methodology proposed by (Thoraval et al, 2004) to compute the equivalents tensors describing the hydromechanical behavior of each block (fig. 6). The results are gathered in table 2. As expected, the equivalent properties are varied according to the number of fractures explicitly included in the models.

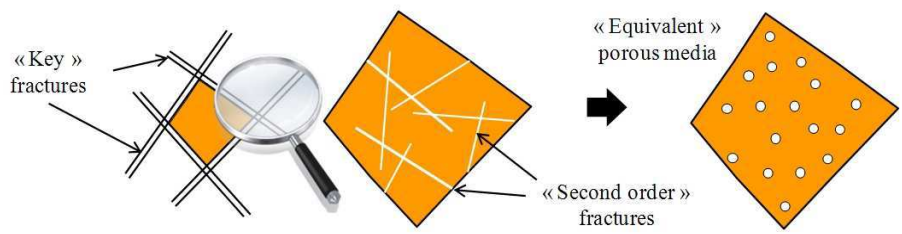

Figure 6. *Illustration of the up-scaling methodology applied to the blocks cut by the "key" fractures*

Geometry	Main fractures (explicitly included)	Other fractures (to be up-scaled)	Equivalents tensors (FLAC3D reference) describing the hydro-mechanical behavior of the up-scaled fractures	
			T_{ijkl} (10^9 MPa)	K_{ij} (10^{-6} m/s)
C' 	All the fractures	None	53,8 23,1 23,1 0,0 0,0 0,0 53,8 23,1 0,0 0,0 0,0 53,8 0,0 0,0 0,0 30,8 0,0 0,0 30,8 0,0 30,8	Intact limestone permeability (10^{-8} m/s) (assumed isotropic)
B' 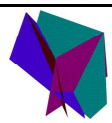	F_2 R_{9a}, J_2, D_6	All the bedding planes	28,7 17,3 18,5 -4,2 5,2 -4,5 39,5 17,1 -10,3 -0,3 7,3 38,3 1,7 10,8 6,2 21,9 -3,8 3,2 23,3 -0,9 24,2	0,103 -0,13 0,131 0,481 0,119 0,343
A' 	F_2	All the fractures excepted F_2	17,6 9,1 9,4 -1,4 0,5 -1,9 19,9 10,5 -1,5 0,8 5,4 14,2 0,2 1,1 1,4 9,4 -0,5 1,7 7,5 0,5 11,5	21,86 -0,49 0,248 19,23 3,63 8,388

(The 4th rank tensor T_{ijkl} links the stress tensor σ_{ij} and the elastic strain tensor ε_{kl}.
The 2nd rank tensor K_{ij} links the fluid flow Q_i and the hydraulic gradient J_j)

Table 2. *Up-scaled hydro-mechanical properties for different models geometries*

3.2.2. *Impact of the intact rock-mass porosity/ permeability*

Several models with different values of matrix porosity and permeability were tested to estimate the influence of the matrix hydraulic properties on the hydromechanical processes in the porous reservoir of the fracture. The results show that the discrepancies with the reference model that includes an "impermeable matrix" remain under 1 % as long as the rock-mass permeability remains smaller than 1×10^{-15} m^2 (the permeability of the Coaraze limestone). If the rock-mass permeability increases up to 1×10^{-13} m^2, then the discrepancies reach 15 %.

3.2.3. *Impact of up-scaling on the prediction of the double-porosity hydromechanical model*

Three models/ geometries were run, with a progressive decrease in the number of selected "key" fractures: model A' with only the injected fracture (F_2), model B' where the vertical fractures R_{9a}, J_2 and D_6 are included, and the reference model C'. Three models (A, B and C) with impermeable blocks were also run, to compare the effects of the up-scaling protocol on the rock-mass hydromechanical response.

Up-scaling tends to reduce the differences between the hydraulic responses calculated for the various runs, as this compensates for not explicitly taking into account all of the fractures. Indeed, as we can see in table 3, the differences between the reference model C' (= C) and models A' and A, with and without up-scaling, respectively, increase from 5 % to 15 %.

Geometry A: F_2 **Geometry B**: F_2, R_{9a}, J_2 et D_6 **Geometry C**: all the fracture		**Computed values at HM_1**			**Computed values at HM_2**	
		Flow rate	**Hydraulic pressure variation**	**Normal displacement variation**	**Hydraulic pressure variation**	**Normal displacement variation**
No up-scaling (with impermeable "matrix")						
1srt injection stage	**A**	0.6571	+34	0.5466	+11.23	0.2044
	B	0.8126		0.4815	+9.13	0.165
	C	0.747		0.432	+9.31	0.157
2nd injection stage	**A**	1.421	+76	1.191	+26.23	0.4467
	B	1.764		1.086	+21.55	0.3817
	C	1.616		0.952	+21.39	0.362
With up-scaling (* in the case **C'**, the matrix permeability is $k=10^{-16}$ m^2)						
1srt injection stage	**A'**	0.8479	+34	0.4768	+7.78	0.1002
	B'	0.8144		0.527	+9.04	0.1663
	C'	0.750		0.430	+9.28	0.157
2nd injection stage	**A'**	1.835	+76	1.155	+18.72	0.2736
	B'	1.807		1.18	+20.24	0.3701
	C'*	1.617		0.951	+21.37	0.362

Table 3. *FLAC^{3D} computed pressure and normal displacement for different up-scaled models*

Going from model A (without up-scaling) to model A' (with up-scaling), figure 7 also shows an important decreasing in the hydraulic pressures (compare figures 7a and 7b) and normal displacements (compare figures 7e and 7f) around the injected point. So, up-scaling appears to be necessary when F_2 is the only fracture included in model A'. In this case, the calculated equivalent permeability is important enough (approximately 2×10^{-5} m/s) to induce a faster reduction in the hydraulic pressures around point HM_1, as well as an increase in the injection flow rate at this point.

With a minimal number of "key" fractures, up-scaling does not appear to be so necessary. The hydraulic response of the instrumented fracture with or without up-scaling is less than a 5 % different between models B and B'. This can be explained considering that in these cases, the equivalent permeability of the blocks remains low (5×10^{-7} m/s) in comparison with the fracture permeability (10^{-3} m/s to 10^{-5} m/s). The same results are obtained on the mechanical response of the fracture. Including the fractures in models B or B', as compared to models A or A', reduces the maximum mechanical opening of fracture F_2 by 17 % without up-scaling, and by 6 % with up-scaling. In conclusion, it appears that including some additional fractures connected to fracture F_2 in the model allows the correct prediction of the F_2 hydromechanical response with or without up-scaling.

Comparisons of figures 7b and 7d show that the hydraulic pressure field into the injected fracture is not impacted upon so much by the model geometry, as long as the fractures excluded are up-scaled. The results are confirmed by comparisons of the normal displacement field into the injected fracture, as shown in figures 7f and 7h.

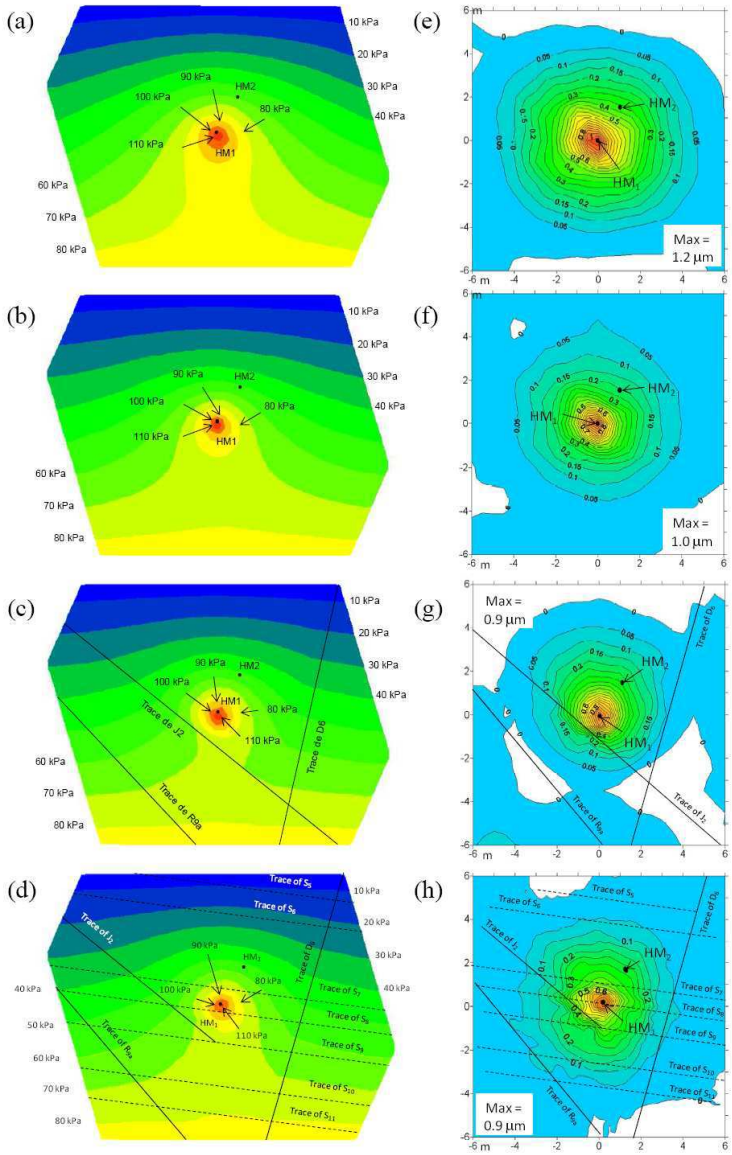

Figure 7. *Calculated hydraulic pressure and normal displacement fields within the injected fracture for the different FLAC3D models geometries; (a) model A - hydraulic pressure; (b) model A' - hydraulic pressure; (c) model B' - hydraulic pressure; (d) model C' - hydraulic pressure; (e) model A - normal displacement; (f) model A' - normal displacement; (g) model B' - normal displacement; (h) model C' - normal displacement*

4. Discussion

This study is based on original measurements carried out at the experimental site of Coaraze, which is a low porosity fractured carbonate reservoir. It is reasonable to ask if the results obtained can be used to characterize and predict hydromechanical behaviors of other sites with different geologies, and in different contexts (unstable rocky slopes, quarries, underground storage).

The input data needed to predict the hydromechanical behavior of the site comprise geological, geometrical, mechanical and hydraulic data. The geological site characterization benefited from the original high accuracy fracture mapping with electronic distance-meter measurements that allowed the location of the fractures in three-dimensional space. This technique appears complementary to the traditional method, the so-called "scanline" method, which only makes it possible to determine the average characteristics (orientation, spacing or density) of the various fracture sets. Since the impact of the main fractures on the hydromechanical predictions is very important, it appears necessary to proceed to this level of accuracy for the measurement of the 3D location of the fractures. For the Coaraze site, the main fractures belong to the sub-vertical discontinuities set, the fractures of which are more permeable and deformable. For unstable rocky slopes or quarries, the main fractures might be the potential slip surfaces, and for underground storage, the main fractures might be the preferential flow pathways. In each case, an expert will have to identify these main fractures according to the context and the goals of any study.

The modeling carried out in this study was based on conceptual models representing the hydraulic, mechanical and hydromechanical behaviors of the fractures and the porous rock matrix. In each model, some parameters had to be estimated using in-situ or laboratory tests. It seems relevant to base the general evaluation on a "traditional" characterization for the rock matrix and for the fracture sets. In more detail, and according to the quality of the prediction that is required, a more accurate and complete characterization might be necessary for some major discontinuities. For this purpose, the use of a removable poroelastic probe that allows synchronous measurements of the fluid pressure and deformations (as we did at Coaraze) is crucial for the determination of the fracture permeability, the stiffnesses and the hydromechanical coupling relationships. In some given contexts (e.g. an underground storage context), the hydromechanical coupled effects might be essential for flow and stability prediction.

Before building a model, it is necessary to clearly identify its goals and the context in which it will be used. Indeed, the degrees of complexity included (or, on the contrary, the simplifications allowed) depend on the possibility of neglecting, simplifying or up-scaling some of that complexity without being able to question the relevance of the results obtained. If we look at stability or flow predictions at a very large scale, it is not possible to take into account all of the fractures in an explicit way (because of limitations in fracture measuring and in numerical modeling). Besides, it is not necessary to do this. Studies have shown that the use of an up-

scaling technique can allow calculation of the hydromechanical characteristics of an equivalent continuous porous medium, and then the correct prediction of the hydromechanical behavior without explicitly introducing the fractures. The technique used in the present study was based on numerical modeling of the response to various hydromechanical loads of the zone to be up-scaled. It can be replaced, if need be, by the application of analytical formulations (e.g. as those of Oda, 1986), in particular if the fracture to be up-scaled is known in an statistical way. It is believed that it is difficult for practical reasons to explicitly introduce all of the existing fractures into the model, and it is advisable to find a way to preserve a limited number of fractures while the other fractures are up-scaled. In-situ hydromechanical testing of the fractures can then help to choose the most permeable or deformable fractures.

At the same time, it is advisable to choose a computer code that can take into account the geometry (simplified or up-scaled), as well as the physical phenomena, retained after analysis of the context and the objectives. An important limiting factor is whether there is the need or not of a model in three dimensions. The codes used within the framework of this study cover the following various cases. If the fractured rock mass can be completely up-scaled, any code that can simulate the hydromechanical behavior of a porous medium can be used. If the fractured rock mass can be replaced by a fracture network cutting out an impermeable matrix, any code simulating the hydromechanical fracture behavior will be appropriate, such as 3DEC for example. In the most complex cases, where the fractured rock mass is replaced by a double porosity medium made up of some major fractures and an equivalent porous medium, the choice of codes is reduced. Within the framework of this study, we adapted the FLAC^{3D} software to this need.

5. Conclusion

Fractured rock masses are often treated as equivalent continua for large-scale analyses, as the fractures in rock masses in practical problems are often too numerous to be represented explicitly in computer models. Proper approaches of correct homogenization and up-scaling are then needed to derive these equivalent properties, with both numerical reliability and capacity to simulate the processes of stress, deformation and fluid flow in fractured rock masses. In the present study, we have examined the possible simplifications and up-scaling that can be carried out to accurately represent the geometry of the porous and fractured rock mass, and to predict its hydromechanical behavior at various scales. A combined discrete and continuum modeling approach is presented. The procedures for determining the equivalent mechanical and hydraulic properties of fractured rock masses are introduced.

The main results of our study can be summarized as follows:

– we developed three-dimensional numerical models to simulate the hydromechanical behavior of some major fractures, as well as the hydromechanical behavior of an equivalent continuous and porous medium that represents the intact rock and the other microfractures;

– the hydromechanical response of the fracture to a hydraulic load (injection/ pumping) does not only depend on the intrinsic characteristics of this fracture, but also on the characteristics of the matrix and of the surrounding fractures. The prediction of the behavior of the injected fracture requires taking into account the fracture surroundings (explicitly or by up-scaling);

– it appears that including some additional fractures in the model that are connected to the injected fracture can allows correct prediction of the hydromechanical response with or without up-scaling. Up-scaling is needed only if no additional fracture is included. This conclusion might however be different in the case of a very-long-duration test.

6. Bibliographie

Ababou, R., 1991. « Approach to large scale unsaturated flow in heterogeneous stratified and fractured geologic media », Report NUREG/CG-5743, US. Nuclear Regulatory Commission, Washington DC, 1991.

Biot, M.A., « General theory of three-dimensional consolidation », *J. Appl. Phys. 12,* 1941, p.155-164.

Blum, P., Mackay, R., Riley, M.S., « Stochastic simulations of regional scale advective transport in fractured rock masses using block upscaled hydro-mechanical rock property data », *Journal of Hydrology 369,* 2009, p. 318-325.

Cappa, F., Guglielmi, Y., Fénart, P., Merrien-Soukatchoff, V., Thoraval, A., « Hydromechanical interactions in a fractured carbonate reservoir inferred from hydraulic and mechanical measurements », *Int. J. Rock. Mech. Min. Sc. 42,* 2005, p. 287-306.

Cappa, F., « Role of fluids in the hydromechanical behavior of heterogeneous fractured rocks: in-situ characterization and numerical modeling », *Bull. Eng. Geol. Env. 65,* 2006, p. 321-337.

Cappa, F., Guglielmi, Y., Gaffet, S., Lancon, H., Lamarque, I., « Use of in situ fiber optic sensors to characterize highly heterogeneous elastic displacement fields in fractured rocks », *Int. J. Rock. Mech. Min. Sc. 43,* 2006-a, 647-654.

Cappa, F., Guglielmi, Y., Rutqvist, J., Tsang, C.F., Thoraval, A., « Hydromechanical modelling of pulse tests that measure fluid pressure and fracture normal displacement at the Coaraze laboratory site, France », *Int. J. Rock. Mech. Min. Sc. 43,* 2006-b, *p. 1062-1082.*

Cappa, F., Guglielmi, Y., Rutqvist, J., Tsang, C.F., Thoraval, A., « Estimation of fracture flow parameters through numerical analysis of hydro-mechanical pressure pulses », *Water Resources Research 44, W11408, doi:10.1029/2008WR007015*, 2008.

Guglielmi, Y., « Apport de la mesure des couplages hydromécaniques à la connaissance hydrogéologique des réservoirs fissurés: approche sur le site expérimental », Habilitation à diriger des Recherche, Université de Franche-Comté, Janvier 1999.

Guglielmi, Y., Cappa, F., Rutqvist, J., Tsang, C.F., Thoraval, A, « Mesoscale characterization of coupled hydro-mechanical behavior of a fractured-porous slope in response to free water-surface movement », *Int. J. Rock. Mech. Min. Sc. 45,* 2008, p. 862-878.

Itasca Consulting Group. Inc., « 3DEC 3-Dimensional Distinct Element Code - Version 1.5: Volume I: User's Manual - Volume II: Verification Problems and Example Applications », Minneapolis, Minnesota: ICG, 1994.

Itasca Consulting Group Inc., « FLAC^{3D} (Fast Lagrangian Analysis of Continua in 3 Dimensions), Version 2.1 », Minneapolis, Minnesota: ICG, 2002.

Min, K.B., Jing, L., Stephansson, O., « Determining the Equivalent Permeability Tensor for Fractured Rock Masses Using a Stochastic REV Approach: Method and Application to the Field Data from Sellafield, UK », *Hydrogeology Journal 12,* 2004, p. 497-510.

Oda, M., « An equivalent continuum model for coupled stress and fluid flow analysis in joint rock masses », *Water Resources Research 22,* 1986, p. 1845-1856.

Pouya, A., Fouché, O., « Permeability of 3D discontinuity networks: New tensors from boundary-conditioned homogenization », *Advances in Water Resources 32,* 2009, p. 303-314.

Terzaghi, K., « *Die Berechning der Durchlässigkeitziffer des Tonesaus dem Verlauf Spannungserscheinungen* », Akad. Der Wissenchafen in Wien, Sitzungsberichte, Mathematischnaturwissenschafttliche Klasse, Part IIA, 142(3/4), 1923, p. 125–138.

Thoraval, A., Renaud, V., « Hydro-mechanical upcaling of a fractured rockmass using A 3D numerical approach, Coupled Thermo-Hydro-Mechanical-Chemical processes in Geo-Systems - Fundamentals, Modelling, Experiments and Applications », *Edited by Ove Stephansson, John A. Hudson and L. Jing. Elsevier Geo-Engineering Book Series. Series Editor; John Hudson, volume 2,* 2004, p. 275-280.

Witherspoon, P.A., Wang, J.S.Y., Iwai, K., Gale, J.E., « Validity of cubic law for fluid flow in a deformable rock fracture », *Water Resources Research 16,* 1980, p. 1016-1024.